ELSEVIER

Colloids and Surfaces A: Physicochem. Eng. Aspects 264 (2005) 157–165

COLLOIDS AND SURFACES A

www.elsevier.com/locate/colsurfa

The influence of electrolyte ions on the interaction forces between polystyrene surfaces

Astrid Drechsler*, Karina Grundke

Leibniz Institute of Polymer Research Dresden e.V., Hohe Strasse 6, 01069 Dresden, Germany

Received 10 August 2004; received in revised form 19 April 2005; accepted 6 May 2005
Available online 16 August 2005

Abstract

The forces between a flat polystyrene film and a polystyrene sphere have been measured in water and solutions of KCl and KOH. All force–distance curves show at distances >5–50 nm an electrical double-layer repulsion whose range and strength depend on the electrolyte concentration. The electrical double-layer potential at the polystyrene surface coincides with its zeta potential. An attractive force of variable range and strength dominates at shorter distances in water, KCl concentrations up to 10^{-2} M and a 10^{-5} M KOH solution. We attribute it to the existence of air nanobubbles on the polymer surface. It is not affected by the KCl concentration. In KOH concentrations $\geq 10^{-4}$ M, the attraction disappears. Instead, an additional "soft" steric repulsion occurs at distances <5–20 nm.

Keywords: Surface forces; Polystyrene; Electrolytes; Nanobubbles; Atomic force microscopy; Zeta potential; Contact angle

1. Introduction

Wetting and adhesion phenomena are strongly influenced by adsorption processes. The adsorption of surfactants and polyelectrolytes from aqueous solutions is frequently used to modify the surface properties of polymers and other materials [1]. But also the adsorption of inorganic electrolyte ions on unpolar surfaces due to dispersion forces influences many phenomena in colloid and interface science [2]. Adsorbed electrolyte ions are, e.g. the origin of the zeta potential of primarily uncharged polymers in aqueous solutions [3,4]. They are able to modify the interactions of polymer surfaces in solutions (e.g. [3,5–7]).

In the last decade, the interaction forces between polymer surfaces in aqueous media have been the object of many publications. They were investigated with the surface force apparatus (SFA) [8–10] and the bimorph surface force apparatus (MASIF) [11–15]. Since the introduction of the colloid probe technique by Butt [16] and Ducker et al. [17], the atomic force microscope (AFM) has become the standard tool for determining the forces between polymers. Colloid probe technique means that the silicon or silicon nitride tip of the AFM cantilever is replaced by a spherical colloidal particle. It allows not only the use of polymer particles as probes but also a qualitative analysis of the data independently of the size of the particle.

Forces have been measured in different symmetric polymer–polymer systems: between polydimethylsiloxane films [8], various polystyrene [14,18–21], polypropylene [5] and Teflon AF surfaces [22]. As intervening media, water and electrolyte solutions of different concentration [5,14,19–21] or various solvents of different polarity [22] have been applied. A systematic investigation of the influence of the electrolyte concentration was done by few authors [15,19–21,23]. In addition, there are studies on the influence of the electrolyte concentration and the pH value on the forces between polypropylene [24] or Teflon AF [7] surfaces and a silica sphere.

These investigations yielded contradictory results. In most of the force–distance curves, but not always, an electrostatic repulsion was found at adequate distance between the inter-

* Corresponding author. Present address: Institut für Polymerforschung Dresden e.V., Postfach 12 04 11, D-01005 Dresden, Germany.
Tel.: +49 351 4658 540; fax: +49 351 4658 284.
E-mail address: drechsler@ipfdd.de (A. Drechsler).

0927-7757/$ – see front matter © 2005 Published by Elsevier B.V.
doi:10.1016/j.colsurfa.2005.05.001

acting surfaces. It is caused by the formation of an electrical double-layer (EDL) of ions adsorbed at the polymer surface. These generate an EDL potential, ψ. Between two planar plates, ψ follows the one-dimensional Poisson–Boltzman equation [25,26]:

$$\frac{d^2\psi}{dx^2} = -\frac{e}{\varepsilon\varepsilon_0}\sum_i z_i\rho_{i\infty}\ \exp\left(\frac{-z_i e\psi}{kT}\right) \quad (1)$$

Here, x is the position between the plates, e the elemental charge, ε and ε_0 the relative permittivity of the solution and the permittivity of vacuum, respectively, k the Boltzmann constant, T the absolute temperature and $\rho_{i\infty}$ is the bulk number density of the ith ion with a valence z_i. From the potential, ψ, the free interaction energy per unit area, V_A, can be derived as described in detail in Ref. [27]. It decays roughly exponentially with increasing distance between the surfaces.

In AFM direct force measurements, the force between a flat surface and a colloidal sphere is measured. For this geometry, the free interaction energy per unit area, V_A, can be derived from the force, F, for each distance, d, between sphere and plane using the Derjaguin approximation [28]:

$$V_A(d) \approx \frac{F(d)}{2\pi R} \quad (2)$$

where R is the radius of the colloidal probe.

In the polymer systems, the EDL interaction is affected by the electrolyte concentration. On one hand, the surface charge and potential of the polymer is modified by adsorbed ions [7,15,19,20,23,24]. In a recent paper, we showed that the surface potential of the polymer calculated from the EDL interaction correlates with the zeta potential obtained by electrokinetic measurements [7]. On the other hand, the exponential decay length of the EDL interaction, the so-called Debye length, is determined by the free ion density in the solution [25].

Near the surface, the force between hydrophobic polymers is dominated by an attractive interaction. Its range reaches from 10 to 30 nm between polypropylene surfaces in NaCl solutions [5] and between polystyrene spheres in (degassed) water [14,18,20] up to 150 nm between polystyrene in non-degassed water [20] and to even 500 nm between very hydrophobic Teflon AF 1600 surfaces in non-degassed water [22]. No systematic influence of the electrolyte concentration on the attractive force was observed. In some investigations [5,19], no effect of the electrolyte was observed. Considine et al. [20] found that the attraction changes randomly with increasing concentration, Kokkoli and Zukoski [23] observed an increase of range and strength of the attraction when the concentration of various electrolytes was raised. Vinogradova et al. [21] revealed two types of force–distance curves between polystyrene surfaces in KCl solutions: one with an attraction as described above and the other a pure electrostatic repulsion. Both types occurred in KCl concentrations $\leq 10^{-4}$ M. In force measurements between polymers and silica spheres or silicon nitride AFM tips, it was found that KCl and NaCl had no influence on the attraction but the increase of the KOH concentration or pH value or the addition of Na_3PO_4 reduces the attractive force significantly [3,6,7,24]. Some scientists observed that the range of the attractive interaction can be reduced by degassing the solutions [5,20].

One origin of attractive forces is the van der Waals force. It can be calculated for sphere–plane geometries using the Hamaker equation [25]:

$$\frac{F}{R} = -\frac{A_{123}}{6d^2} \quad (3)$$

A_{123} is the non-retarded Hamaker constant of the system, a specific material constant. For polymers, the van der Waals force decays within a range of 5–10 nm [5,7,18]. An attractive force of this range was found in asymmetric systems when a hydrophobic polymer surface interacted with a hydrophilic silica sphere [7,24].

In symmetric hydrophobic polymer–polymer systems, the attraction is usually stronger. An attractive interaction of widely varying range and strenght was frequently found between hydrophobic surfaces. Therefore, it is called the "hydrophobic interaction" [29]. Many scientists tried to explain the origin of this force. Some attribute it to a perturbation in the ordering of water propagating through the liquid [30] or to different kinds of electrostatic interactions [12]. There is much evidence that it is in many cases due to the presence of sub-microscopic bubbles (nanobubbles) adhered to the surface. This proposal bases on the observation of steps or discontiuities in the force–distance curves when the probe was approached to the surface. The steps are interpreted as bridging of multiple bubbles [12]. This assumption is supported by the fact that the force can be reduced when the solutions are degassed [5,20,31,32] and is not measured between surfaces that had never been exposed to air [10,31,32]. Bubble-like domains of 20–30 nm height have been visualized on hydrophobized silica surfaces [32–35]. On polystyrene, bubbles of 5–12 nm size have been detected whose number and size is reduced in degassed water [36]. Force measurements between silica spheres and air bubbles in aqueous solutions [37–40] showed that hydrophilic spheres were repelled by the bubbles; hydrophobized or hydrophobically contaminated spheres were attracted and penetrated the bubbles. Polystyrene spheres were attracted by air bubbles [21].

The weakening of the attractive force in polymer systems at high pH values has been interpreted in terms of the preferential adsorption of OH^- ions [7] as revealed by zeta potential measurements [3,4,41] but could not be fully explained.

For practical purposes, it is of interest if changes in the interaction forces can be correlated to a variation of the interfacial free energy at the solid–liquid interface that can be determined by measuring the liquid contact angle. Several authors [23,42–45] found that the contact angle of unpolar polymers or other hydrophobic surfaces without ionizable

groups is not affected by simple ions or variation of the pH value. Only Butkus and Grasso [46] reported a slight increase in water contact angles on paraffin wax, PTFE and polyethylene with increasing NaCl concentration.

As outlined above, the influence of electrolyte solutions on the interactions between hydrophobic polymers has not been clarified sufficiently. In a first step, it is necessary to elucidate relations between the adsorbability of the electrolyte ions and the forces between the surfaces. In this work, direct force measurements were performed between two equivalent polymer surfaces and compared with the results of zeta potential and contact angle measurements providing information about the adsorption of ions at the polymer/liquid interface. We used the model polymer polystyrene because a lot of knowledge about the surface properties of this polymer is available and several direct force measurements with contradictory results have been done [14,18–21]. This study examines systematically the effect of differently adsorbing ions as K^+, Cl^- and OH^-. Of special interest is if there is a "hydrophobic interaction" and how it is affected by the electrolytes. To reduce the influence of air bubbles, the solutions were degassed. During the measurement, air contact could not be avoided completely.

2. Experimental

2.1. Polymer surfaces

Homogeneous films of polystyrene were prepared by spin-coating a 2% solution of polystyrene 148 H (BASF, Germany) in THF (≥99.5%, Fluka, Switzerland) onto silicon wafers at room temperature with a spin rate of 4000 rpm for 15 s. A commercial spin-coater P6708 (Speedline Technologies, IN, USA) was used. Prior to spin-coating, the wafers had been cleaned with chromosulphuric acid and hydrogen peroxide. In some cases, they have been hydrophobized by exposure to 1,1,1,3,3,3-hexamethyldisilazane (99.9%, Sigma–Aldrich GmbH, Germany) vapor in order to improve the adhesion of the polymer films. This procedure did not affect the contact angle of water on the polystyrene film. The advancing angles are in the range of 88–95°, the receding angles lie between 70° and 76°. The film thickness determined by ellipsometry is (72 ± 1.5) nm. An atomic force microscopy image of the polystyrene films made with a NanoScope III (Digital Instruments, Santa Barbara, USA) in the tapping mode is given in Fig. 1 (left part). It shows a very smooth surface with a RMS roughness of 0.3 nm covered with singular asperities of up to 800 nm width, up to 50 nm height and a mean distance of about 20 μm. Since the phase image of the cantilever oscillation (Fig. 1, right part) did not reveal a contrast between the flat surface and the asperities they are assumed to be particles or bubbles covered with polystyrene. In AFM images of the polystyrene film made after exposure to water and electrolyte solutions, no change in the morphology was observed.

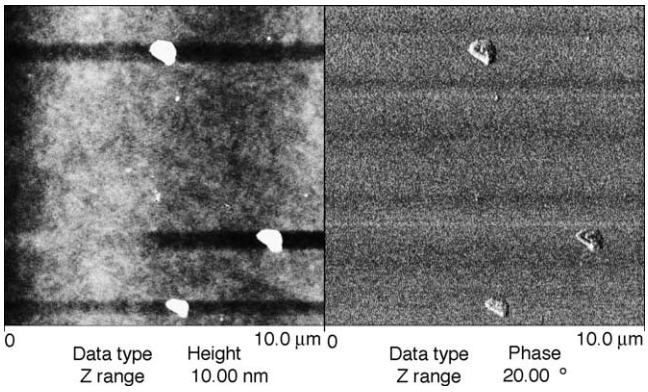

Fig. 1. AFM image of a 10 μm × 10 μm area of the polystyrene film made in tapping mode: height image (left) and phase image (right).

2.2. Electrolyte solutions

Electrolyte solutions have been prepared from KCl (Merck, 99.5%) and KOH (Fluka, 86%) with purified water (specific resistance 18.2 MΩ/cm) taken from a Milli-Q system (Millipore GmbH). To minimize the influence of ions dissolved from the atmosphere, the solutions were degassed 1 h at 100 mbar and stored under nitrogen. Immediately before they were filled into the AFM fluid cell, the solutions were degassed again at 100 mbar for 30–60 min. During the measurements, contact with air could, however, not be avoided.

2.3. Preparation of the colloid probes

Polystyrene microspheres DVB 1–50 μm (Duke Scientific Corp., USA) have been glued onto tipless contact silicon cantilevers CSC12/tipless/50 (MikroMasch, Tallinn, Estonia) as described in detail in Ref. [7]. The spring constant of the cantilevers was determined by the method of Cleveland et al. [47]. For all cantilevers, it was in the range of (0.8 ± 0.2) N/m. The diameter of the spheres was estimated from scanning electron microscopy images. The surface of a polystyrene sphere imaged by AFM using an UltraSharp silicon tip grating TGT 01 (NT-MDT, Russia) is shown in Fig. 2 (left part). The cantilever deflection image (right part) shows that the spheres have a low RMS roughness (1 nm).

2.4. Direct force measurements

The surface force measurements were performed at room temperature using a commercial atomic force microscope Multi Mode® (Digital Instruments, Santa Barbara, CA, USA) equipped with a standard fluid cell. Each measurement series started with a measurement in degassed purified water. Then, the electrolyte concentration was increased stepwise by rinsing the cell with 15 ml of the freshly degassed solution without intermediate air contact. Immediately after the cell had been filled, the cantilever was approached stepwise to the sur-

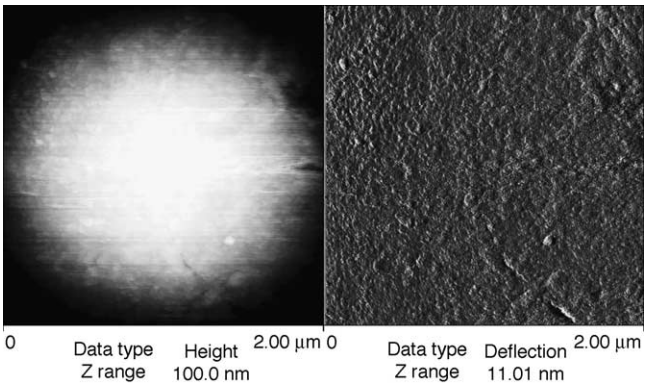

Fig. 2. AFM image of a 3 mm × 3 mm area of a polystyrene sphere obtained with an ultrasharp silicon tip grating: height image (left) and cantilever deflection image (right).

face. During 60 min, a number of force curves was recorded on different points of the surface to avoid artefacts caused by asperities and possible damaging of the surface.

A detailed description of force measurements with an AFM is given, e.g. in Refs. [41,48]. The raw data were converted to force–distance curves as described by Senden [49]. The deflection measured at large distances from the surface was defined as zero deflection; the linear slope at the highest applied force in water was taken as the compliance region to adjust the sensitivity of the detector and the point of zero distance. This assumption might cause errors because it cannot be checked whether this slope represents truly a direct, inelastic contact between the two surfaces. Forces were calculated by multiplying the deflection d by the spring constant k of the cantilever.

Since the attractive forces are affected by the approach velocity of the sphere and the maximum applied load (cf. [14,35]), both values have usually been kept constant.

2.5. Contact angle measurements

Advancing and receding contact angles of water and electrolyte solutions on the polystyrene films were determined using a sessile drop method based on a conventional goniometer technique (DSA 10, Krüss GmbH, Germany). The accuracy of this technique is in the range of $\pm 2^{\circ}$.

3. Results and discussion

3.1. Force measurements in KCl solutions

We did several series of force–distance measurements between polystyrene spheres and flat polystyrene films each starting in water and stepwise increasing the KCl concentration from 10^{-5} or 10^{-4} to 10^{-2} M. In Fig. 3, force–distance curves are shown that have been measured with a sphere of (9 ± 1) µm diameter on approach in water and three different KCl solutions. All curves plotted in Fig. 3 are from

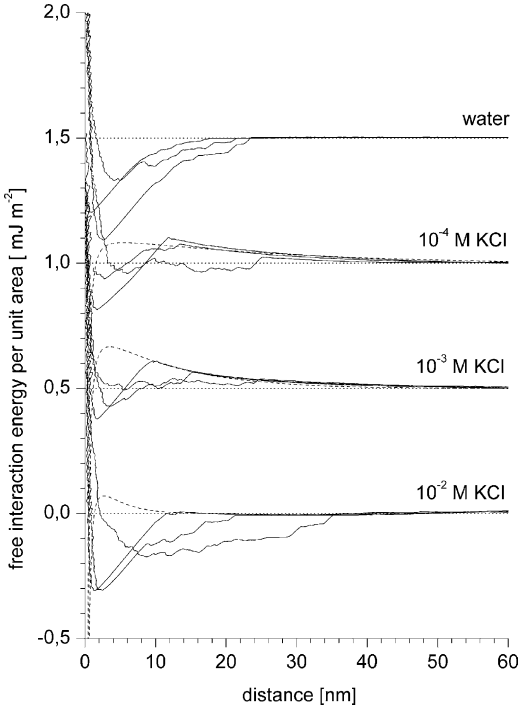

Fig. 3. Interaction free energy per unit area curves measured on approach between a polystyrene sphere and a flat film in water and KCl solutions. The solid lines give the experimentally measured curves, the dashed lines the theoretical EDL and van der Waals interaction. The curves for different concentrations are shifted in vertical direction.

the same measurement series. For each concentration, three curves have been selected that represent the variations that occurred in the large number of curves measured at different times and surface points. The data are not averaged or smoothed. For clarity, the curves are shifted in vertical direction; dotted lines give the zero point of the free interaction energy. The vertical scale gives the data in terms of the free interaction energy per unit area, V_A in a logarithmic scale. V_A was calculated according to Eq. (2) using the sphere radius $R = 4.5$ µm and a spring constant of the cantilever $k = 0.8$ N/m. The uncertainties in the determination of the radius and the spring constant (cf. Section 2) cause a systematic error of V_A of about 10% which is, however, for all curves the same.

Most of the force–distance curves measured in the same solution coincide for large distances (>30 nm). In water, no force acts in this range. In 10^{-4} and 10^{-3} M KCl solutions, a repulsive force is visible that grows exponentially with decreasing distance between the sphere and the flat film. This part of the curves has been modelled as a solution of the Poisson–Boltzmann equation (Eq. (1)). The dashed lines in Fig. 3 represent these model curves including the contribution of the van der Waals force. A good fit of the experimentally determined curves was obtained using the zeta potential of polystyrene measured by Zimmermann [50] as constant surface potentials in the modelling. The potential values are given in Table 1. The zeta potential is the electric potential at the shear plane between the immobile and the mobile ion adsorption layer of a solid surface [4,26]. From the coinci-

Table 1
Surface potential values used to fit the EDL interaction between polystyrene surfaces in KCl and KOH solutions and zeta potential of polystyrene (from Ref. [50])

Electrolyte concentration (mol/l)	Surface potential in KCl (mV)	Zeta potential in KCl (mV)	Surface potential in KOH (mV)	Zeta potential in KOH (mV)
10^{-5}	–	–	–	−110
10^{-4}	−60	−60	−80	−95
10^{-3}	−50	−50	−70	−70[a]
10^{-2}	−28	−28[a]		
1.2×10^{-2}			−52	–

[a] Values extrapolated from the zeta potential curves in Ref. [50].

dence of the zeta potential and the surface potential obtained by fitting our force–distance curves we conclude that the repulsive force is an electrical double-layer (EDL) interaction caused by the charging of the polystyrene surfaces by adsorbed ions. In 10^{-2} M KCl solution, no repulsive interaction was observed at distances >10 nm. The model curve in Fig. 3 for this concentration that was calculated assuming a surface potential of −28 mV, shows that an EDL interaction would decay within a range of 10 nm because it is screened by the free ions in the solution. In the experimentally measured curve, in this distance range a strong negative, i.e. attractive force dominates.

This attractive force has been observed in all KCl solutions. The superposition of the long-range repulsive EDL interaction and a short-range attraction leads to a maximum of the interaction energy at a certain distance from the surface. If in AFM force measurements the sphere crosses this repulsive barrier, the tension of the cantilever spring caused by the repulsive force leads to a mechanical instability, the sphere jumps into contact with the surface. Vice versa, if the sphere is retracted from the surface, it keeps adhered by the attractive force until the force applied by the cantilever exceeds the adhesion force. Then, the sphere jumps suddenly out of contact. The distance where the jump into contact happens, the jump-in distance, is a measure for the range of the attractive force. From the jump-out distance, the adhesion force, i.e. the strength of the attraction, can be calculated by extrapolating the jump-out line to the point of intersection with the *y*-axis, i.e. by multiplying the jump-out distance by the spring constant of the cantilever [35]. While the jump-in distance shows the range of the attraction, the jump-out distance is a measure for its strength.

As can be seen from Fig. 3, in water and all KCl solutions up to a concentration of 10^{-2} M a first jump-in occurs at a distance between 10 and 35 nm. Often not a straight jump into contact was observed but a stepwise motion towards the surface. This refers to several little jumps into intermediate force minima but not to one distinct adhesion force. The differences between the jump-in distances measured in one solution are larger than the differences between those determined in various KCl concentrations. The same accounts for the jump out of contact. It often occurred in several steps and differed widely in its width. For comparison, small jumps were neglected. Adhesion forces were calculated from the first, most pronounced jump-out and normalized by $2\pi R$ to get the adhesion free energy per unit area. All data measured in one series and one concentration were averaged. In Fig. 4, these values are plotted. The data given by the solid squares correspond to the curves shown in Fig. 3. There are even larger differences in the range and strength of the attractive interaction comparing the results of several measurement series. Within one measurement series, the jump-out distances are scattered randomly within the range given by the error bars. No systematic effect of the KCl concentration on the adhesion force is visible. Such an unsystematic dependence of the jump-in distance on the electrolyte concentration has been observed also by other authors [5,20].

What is the origin of this attractive force? The van der Waals force calculated according to Eq. (3) using a Hamaker constant of 0.95×10^{-21} J [18,21] is included in the model curves in Fig. 3. It would cause a jump-in at a distance of about 3 nm, i.e. 3–10 times smaller than the jump-in distance measured by us.

The wide scattering of jump-in and jump-out distances and the insensitivity to electrolyte concentration are typical features of the "hydrophobic interaction" caused by air nanobubbles or vapor cavities on the hydrophobic polymer surface [29]. Air nanobubbles on polystyrene surfaces have been detected experimentally [36]. The stepwise approach to the surface is another hint for their existence [12]. It is very

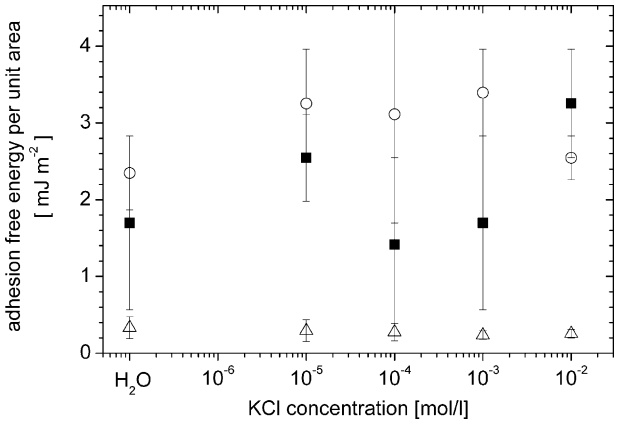

Fig. 4. Average adhesion free energy per unit area measured between polystyrene spheres (spheres and squares: diameter 9 μm; triangles: diameter 13 μm) and a flat polystyrene surface in KCl solutions.

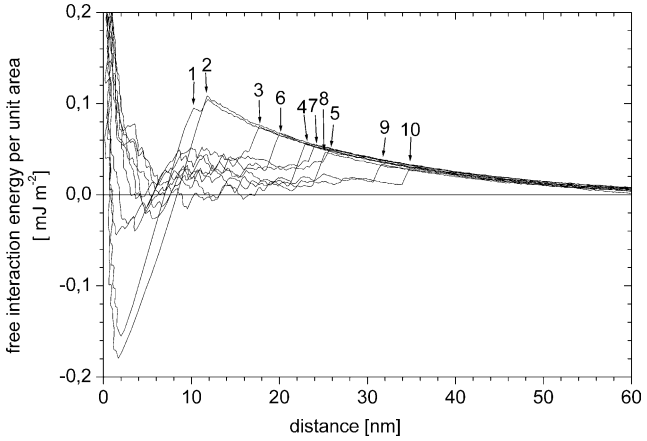

Fig. 5. Interaction free energy per unit area curves measured during 10 successive approaches between polystyrene surfaces in 10^{-4} M KCl solution. The numbered arrows denote the first jump-in the first, second, third, etc. approach.

likely that although the solutions were degassed, air bubbles or a thin air layer have been kept attached to the hydrophobic surface while the fluid cell was filled.

The bridging by nanobubbles is evident in the evolution of the force–distance curves during successive approaches. Fig. 5 shows 10 force–distance curves measured on the same point following each other in time intervals of 3 s. On first and second approach (1, 2), the sphere jumps at a distance of 12 nm directly in contact with the surface. In the following eight approaches, the distance of the first jump-in grows up to 35 nm. The sphere jumps now in many small steps towards the surface until contact is reached. The single steps may be explained as formation of a new three-phase line between the polystyrene sphere, the solution and a bubble. Interestingly, with increasing number of contacts and increasing jump-in distance (cf. Fig. 5), the minimum of the adhesion force becomes less pronounced. Fig. 6 shows the adhesion free energy per unit area measured on retraction after the approaches shown in Fig. 5. The decrease of the adhesion free energy coincides with the shrinking depth of the force

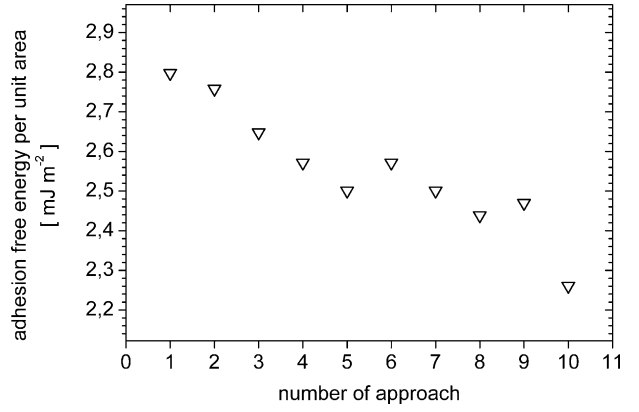

Fig. 6. Average adhesion free energy per unit area measured on retraction after the approaches shown in Fig. 5.

minimum in the approach curves, i.e. with increasing number of contacts the attractive force becomes weaker but of longer range. This indicates that during several approaches of the colloidal sphere the bubbles may be divided into smaller ones [12]. While at first contact the sphere penetrates one bubble of 12 nm size, it enters in the later approaches a cluster of small bubbles. Vice versa, the adhesion force directly in contact with the surface becomes lower but there is a bridging over a longer distance.

All these facts lead to the assumption that the attractive force is most probably caused by air nanobubbles. Presumably, the size of the nanobubbles changes incidentally but is not affected by K^+ or Cl^- ions. Therefore, no influence of the KCl concentration on range and strength of the attractive force was found. The existence of bubbles of variable size causes the adhesion force to be scattered randomly in a wide range. The differences between the adhesions determined in various measurement series can be explained by the fact that at the beginning of the experiment different amounts of air are attached to the surfaces. A slight increase of the adhesion during a measurement series could be due to additional air brought into the cell with a new solution.

If the polystyrene sphere is approached to a distance <2 nm, a steep rise of the force is observed instead of a hard-wall contact. This effect seems not to depend on the electrolyte concentration. It probably represents a steric repulsion caused by compression of the interacting surfaces [5], but also the hysteresis of the piezo positioning system of the AFM and an inaccurate arbitrary definition of the zero distance can cause such an effect.

3.2. Force measurements in KOH solutions

In water and KOH solutions, several series of direct force measurements have been performed. They were all measured with the same sphere as the curves in KCl presented in Fig. 3. The procedure was the same as described in Section 3.1. Fig. 7 shows selected interaction free energy (V_A)–distance curves from one measurement series. V_A was calculated according to Eq. (2) using the sphere radius $R = 4.5$ μm and the approximate spring constant of the cantilever $k = 0.8$ N/m with a systematic error of 10% as described in Section 3.1. For each concentration, up to three characteristic curves have been selected. The data are not averaged or smoothed. For clarity, the curves are shifted in vertical direction.

The force curves measured in water show the features described in Section 3.1: a slight repulsion at distances >20 nm and a stepwise increasing attraction at smaller distances probably representing a bridging between the polystyrene surface and the sphere by small air bubbles. The steep rise of the force–distance curves at distances <2 nm is assumed to be caused by a deformation of the polystyrene surfaces. When the KOH concentration is increased to 10^{-5} M, no significant change in the force–distance curves is observed. This is in contradiction to the strong charging of polystyrene in 10^{-5} M KOH shown in zeta potential measure-

ments [50]. Maybe, the OH^- ion concentration was decreased in our experiments due to contact with air.

Raising the KOH concentration to and above 10^{-4} M leads to a qualitative change of the curves. Now they are dominated by a strong repulsion; no jump into contact takes place. This change was found in all measurement series in KOH solutions independently of the differences between the force and distance curves in the initial measurement in water. Vinogradova et al. [21] measured similar force–distance curves between polystyrene surfaces in KCl solutions. They classified the curves showing a weak repulsion and a strong attraction as type 1, the purely repulsive curves as type 2. While we found curves of type 1 in water, all KCl concentrations and in 10^{-5} M KOH, and curves of type 2 always in KOH concentrations $\geq 10^{-4}$ M, Vinogradova et al. observed curves of type 2 only in KCl concentrations $\leq 10^{-4}$ M simultaneously with curves of type 1. Vinogradova attributes the attractive interaction of type 1 to nanobubbles but gives no explanation for the curves of type 2.

For the curves of type 2, we modelled the EDL interaction as a solution of the Poisson–Boltzmann equation (Eq. (1)). Since no jump-in was observed, the van der Waals force was not taken into account. The model curves are included in Fig. 7. They fit the experimentally determined curves at larger distances (>20 nm in 10^{-4} M, >15 nm in 10^{-3} M and >3 nm in 1.2×10^{-2} M). The surface potential used to fit the curves in 10^{-3} M agrees with the approximate zeta potential value of polystyrene extrapolated from literature data [50]. All potential values are given in Table 1. For 10^{-4} M KOH, the surface potential from our fit is smaller than the zeta potential given by Zimmermann [50]. This might be caused by a contamination of the solution by carbonate ions from air during the measurement or by differences in the surface properties of the polystyrene film and the sphere. There might also be an influence of the incertainty in the arbitrary definition of the zero distance in the AFM force measurement.

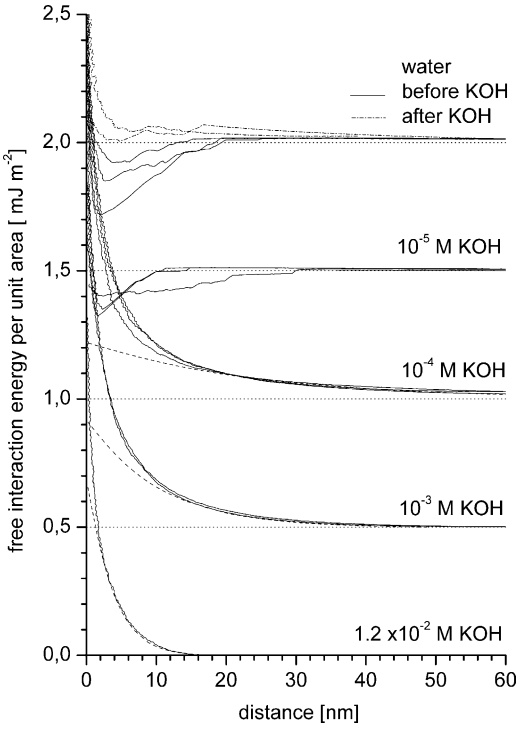

Fig. 7. Interaction free energy per unit area curves measured on approach between a polystyrene sphere and a flat film in water (before and after contact with KOH) and KOH solutions. The solid lines give the experimentally measured curves, the dashed lines the theoretical EDL interaction. The curves for different concentrations are shifted in vertical direction.

In addition to the EDL repulsion, a stronger repulsion at distances <10 nm was observed. Its steep rise indicates a steric interaction. A similar "soft repulsion" has been observed by Carambassis et al. [51] between hydrophobic surfaces in NaCl solutions prior to their jump into contact. They interpret it as a compression of an air nanobubble. Other authors [35,21] challenge this hypothesis but give no other explanation. From zeta potential measurements, it is known that OH^- ions are adsorbed strongly to polymer surfaces as polystyrene or fluorocarbons [3,4]. Therefore, such a "soft" steric repulsion might be attributed to a hydrated layer of OH^- and counterions attached to the surface. Since in our measurements in water and KCl solutions air bubbles play an essential role, we suppose that also in the systems showing force–distance curves of type 2 nanobubbles are present. Fielden et al. [40] reported that air bubbles are charged in electrolyte solutions in a similar way as solid hydrophobic surfaces. Therefore, we assume that the surface potential of the nanobubbles creates a repulsive force that is high enough to prevent penetration by the polystyrene sphere even if the free interaction energy per unit area applied by the sphere exceeds 2 mJ/m^2 but that the air bubbles are compressed by the applied force.

The retraction curves in KOH solutions did not show an abrupt change from attractive to purely repulsive behavior. As can be seen from Fig. 8, the mean values of the adhesion force from all measurement series decrease steadily with increasing KOH concentration. But still in 10^{-3} and 1.2×10^{-2} M solutions often an adhesion of the sphere was found. It caused,

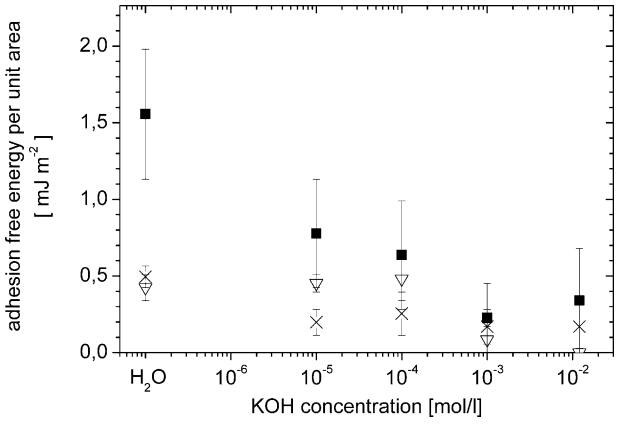

Fig. 8. Average adhesion free energy per unit area measured between a polystyrene sphere (diameter 9 μm) and a flat polystyrene surface in KOH solutions (three measurement series).

however, no distinct jump-out but a delay in the retraction of the sphere.

The reduction of the attractive forces by KOH has already been found in recent direct force measurements between a Teflon AF surface and a silica sphere [7] and in former direct force measurements on polymers. The attractive force between Teflon AF, polystyrene, polypropylene [52] and the fluoropolymer CHF [41], and a silicon nitride tip was weakened by addition of KOH but not affected by KCl. Meagher and Pashley [24] observed a decrease of the jump-in distance between a polypropylene surface and a silica sphere with increasing pH, i.e. with increasing concentration of OH^- ions. Usually, a steady decrease of range and strength of the attraction was found instead of the sudden change observed in the present study.

Weidenhammer and co-workers [3,41] discussed the decreasing attraction with growing OH^- concentration as a result of the competitive interaction between the electrolyte ions, the AFM probe and the polymer surface. The stronger the ion–polymer interaction, the weaker is the probe–polymer attraction. Since OH^- ions are adsorbed much stronger than K^+ or Cl^- ions, they reduce the van der Waals interaction. Above a "critical" concentration no more net attractive interaction is observed.

This explanation can account for the polystyrene–polystyrene system, too. The "critical" concentration is in our case above 10^{-3} M. It is not clear, however, if the surface determining the interaction is the polystyrene surface or the surface of the air nanobubbles. The coincidence between the surface potential obtained from the fits of our data and the zeta potential of polystyrene indicates an interaction between two polystyrene surfaces. But air bubbles are just as polystyrene charged negatively in neutral aqueous solutions [53]. In NaCl solutions, repulsive EDL forces were observed between silica spheres and bubbles being affected by changes of the electrolyte solutions in the same way as the forces measured between solid polymers [40]. Therefore, the force contribution by air bubbles cannot be easily distinguished from that caused by solid hydrophobic surfaces. The "soft" steric repulsion and the adhesion force seen on retraction of the sphere suggest the presence of deformable nanobubbles attracting the polystyrene sphere in close contact.

To test the reversibiliy of the OH^- adsorption, we recorded some force–distance curves following the measurements in KOH solutions after rinsing the fluid cell extensively with water. Some of these curves are shown as dashed lines in the uppermost part of Fig. 7. There is still a slight repulsion, probably because the cell was not rinsed extensively enough to remove all K^+ and OH^- ions. The attractive force is the same as in the initial water measurements. Thus, the qualitative change of the force curves is reversible; no modification of the polystyrene surface occurred. In some measurement series, the attraction became even stronger than in the first measurements in water. Probably during rinsing, additional air bubbles were brought into the cell.

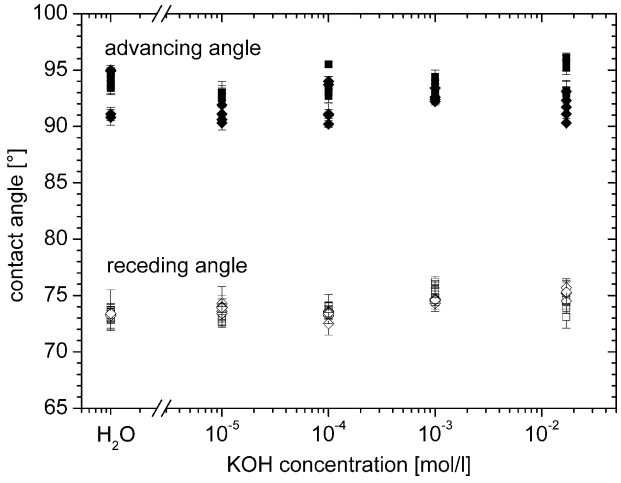

Fig. 9. Advancing and receding contact angles of water and KOH solutions on polystyrene films.

The marked influence of KOH solutions on the interaction forces recommends that it might influence also the wetting behavior of polystyrene. To check this, we performed contact angle measurements with water and KOH solutions on polystyrene films prepared in the same way as those used in the direct force measurements.

Fig. 9 shows the advancing and receding contact angles of water and KOH solutions on polystyrene films. For each concentration, the results of at least three single droplets on different polystyrene samples are given. The advancing angles are in the range of 88–95°, the receding angles lie between 70° and 76°. No influence of the KOH concentration is found within the limits of experimental error. This is in conformity with the results of several other scientists [23,42–45,54]. We also measured the contact angles of polystyrene samples after they had been used in force measurements in KOH solutions. No change was observed.

4. Conclusions

The present study describes direct force measurements between a polystyrene sphere and a flat polystyrene film in aqueous solutions of KCl and KOH. Two different types of force–distance curves have been observed. Type 1 shows a weak electrical double-layer repulsion at distances >15–50 nm. This force contribution can be modelled as solution of the Poisson–Boltzmann equation. The surface potential used in the modelling coincides with the zeta potential of polystyrene. At smaller distances it is superimposed by a strong attraction whose range and strength vary randomly but are not affected systematically by addition of KCl. When the sphere is retracted, adhesion free energies per unit area up to 5 mJ/m^2 are measured. We attribute this attraction to the existence of sub-microscopic air bubbles (nanobubbles) on the hydrophobic polystyrene surface. Force–distance curves of type 1 have been observed in water, all KCl solutions up

to a concentration of 10^{-2} M and in a 10^{-5} M KOH solution. In KOH concentrations $\geq 10^{-4}$ M force–distance curves of type 2 have been measured. They are composed of an electrical double-layer repulsion and a stronger, short-ranged "soft repulsion" acting at distances <5–20 nm. No jump-in as evidence for an attractive force occured. It is assumed that the soft repulsion represents the compression of air nanobubbles. Probably both the nanobubbles and the polystyrene sphere are highly charged by an adsorbed layer of OH^- and counterions. Therefore, they repel each other preventing a jump into contact. On retraction, an adhesion force was observed which was, however, lower than 1 mJ/m^2 and decreased with increasing KOH concentration. Despite the significant influence of KOH solutions on the interaction forces, no change of the solution contact angle on polystyrene was observed within the limits of experimental error.

Acknowledgments

Financial support for this work provided by the Deutsche Forschungsgemeinschaft (LA-818/11-1) is gratefully acknowledged. The authors also would like to thank J. Zhang for the EDLA program to model the force–distance curves, M. Franke for the REM images, N. Petong and C. Froeck for their help to prepare colloid probes and to measure spring constants.

References

[1] H.-J. Jacobasch (Ed.), Surface modification of polymers, Macromol. Symp. 126 (1998).
[2] B.W. Ninham, V. Yaminski, Langmuir 13 (1997) 2097.
[3] P. Weidenhammer, H.-J. Jacobasch, J. Colloid Interface Sci. 180 (1996) 232.
[4] R. Zimmermann, S. Dukhin, C. Werner, J. Phys. Chem. B 105 (2001) 8544.
[5] L. Meagher, V. Craig, Langmuir 10 (1994) 2736.
[6] P. Weidenhammer, Macromol. Symp. 126 (1998) 51.
[7] A. Drechsler, N. Petong, J. Zhang, D.Y. Kwok, K. Grundke, Colloids Surf. A 250 (2004) 357.
[8] J.-E. Proust, E. Perez, Y. Segui, D. Montalan, J. Colloid Interface Sci. 126 (1988) 629.
[9] A. Grabbe, R.G. Horn, J. Colloid Interface Sci. 157 (1993) 375.
[10] J. Wood, R. Sharma, Langmuir 11 (1995) 4797.
[11] J.L. Parker, P.M. Claesson, J.-H. Wang, H.K. Yasuda, Langmuir 10 (1994) 2766.
[12] J.L. Parker, P.M. Claesson, P. Attard, J. Phys. Chem. 98 (1994) 8468.
[13] T. Ederth, K. Tamada, P.M. Claesson, R. Valiokas, R. Colorado Jr., M. Graupe, O.E. Shmakova, T.R. Lee, J. Colloid Interface Sci. 235 (2001) 391.
[14] F.-J. Schmitt, T. Ederth, P. Weidenhammer, P. Claesson, H.-J. Jacobasch, J. Adhes. Sci. Technol. 13 (1999) 79.
[15] J. Frank, A. Janke, F.-J. Schmitt, Macromol. Chem. Phys. 202 (2001) 201.
[16] H.-J. Butt, Biophys. J. 60 (1991) 1438.
[17] W.A. Ducker, T.J. Senden, R.M. Pashley, Langmuir 8 (1992) 1831.
[18] M.E. Karaman, L. Meagher, R.M. Pashley, Langmuir 9 (1993) 1220.
[19] Y.Q. Li, N.J. Tao, J. Pan, A.A. Garcia, S.M. Lindsay, Langmuir 9 (1993) 637.
[20] R.F. Considine, R.A. Hayes, R.G. Horn, Langmuir 15 (1999) 1657.
[21] O.I. Vinogradova, G.E. Yakubov, H.-J. Butt, J. Chem. Phys. 114 (2001) 8124.
[22] R.F. Considine, C.J. Drummond, Langmuir 16 (2000) 631.
[23] E. Kokkoli, C.F. Zukoski, Langmuir 14 (1998) 1189.
[24] L. Meagher, R.M. Pashley, Langmuir 11 (1995) 4019.
[25] J.N. Israelachvili, Intermolecular and Surface Forces, Academic Press, San Diego, 1991.
[26] H.-J. Butt, K. Graf, M. Kappl, Physics and Chemistry of Interfaces, Wiley/VCH, Weinheim, 2003.
[27] J. Zhang, A. Drechsler, K. Grundke, D.Y. Kwok, Colloids Surf. A 242 (2004) 189.
[28] B.V. Derjaguin, Kolloid-Zeitschr. 69 (1934) 155.
[29] H.K. Christenson, P.M. Claesson, Adv. Colloid Interface Sci. 91 (2001) 391.
[30] J.C. Eriksson, S. Ljunggren, P.M. Claesson, J. Chem. Soc., Faraday Trans. 2 (85) (1989) 163.
[31] N. Ishida, M. Sakamoto, M. Miyahara, K. Higashitani, Langmuir 16 (2000) 5681.
[32] M. Sakamoto, Y. Kanda, M. Miyahara, K. Higashitani, Langmuir 18 (2002) 5713.
[33] N. Ishida, T. Inoue, M. Miyahara, K. Higashitani, Langmuir 16 (2000) 6377.
[34] J.W.G. Tyrrell, P. Attard, Phys. Rev. Lett. 87 (2001) 176104.
[35] J.W.G. Tyrrell, P. Attard, Langmuir 18 (2002) 160.
[36] R. Steitz, Th. Gutberlet, Th. Hauss, B. Kloesgen, R. Krastev, S. Schemmel, A.C. Simonsen, G.H. Findenegg, Langmuir 19 (2003) 2409.
[37] H.-J. Butt, J. Colloid Interface Sci. 166 (1994) 109.
[38] M. Preuss, H.-J. Butt, Langmuir 14 (1998) 3164.
[39] W.A. Ducker, Z. Xu, J.N. Israelachvili, Langmuir 10 (1994) 3279.
[40] M.L. Fielden, R.A. Hayes, J. Ralston, Langmuir 12 (1996) 3721.
[41] H.-J. Jacobasch, F. Simon, P. Weidenhammer, Colloid Polym. Sci. 276 (1998) 434.
[42] Z.A. Zhou, H. Hussein, Z. Xu, J. Czarnecki, J.H. Masliyah, J. Colloid Interface Sci. 204 (1998) 324.
[43] N. Arbiter, Y. Fujii, B. Hansen, A. Raja, in: P. Somasundaran, R.B. Grieves (Eds.), Advances in Interfacial Phenomena of Particulate/Solution/Gas Systems Applications to Flotation Research, AIChE Symp. Ser. 150, vol. 71, AIChE, New York, 1975, p. 176.
[44] R. Schweiss, P.B. Welzel, C. Werner, W. Knoll, Langmuir 17 (2001) 4304.
[45] P.B. Welzel, C. Rauwolf, O. Yudin, K. Grundke, J. Colloid Interface Sci. 251 (2002) 101.
[46] M.A. Butkus, D. Grasso, J. Colloid Interface Sci. 200 (1998) 172.
[47] J.P. Cleveland, S. Manne, D. Bocek, P.K. Hansma, Rev. Sci. Instrum. 64 (1993) 403.
[48] H.-J. Butt, in: E. Gileadi, M. Urbakh (Eds.), Encyclopedia of Electrochemistry, vol. 1: Thermodynamics and Electrified Interfaces, Wiley/VCH, Weinheim, 2002, p. 255.
[49] T.J. Senden, Curr. Opin. Colloid Interface Sci. 6 (2001) 95.
[50] R. Zimmermann, Diploma Thesis, Hochschule für Technik und Wirtschaft Mittweida, 1997.
[51] A. Carambassis, L.C. Jonker, P. Attard, M.W. Rutland, Phys. Rev. Lett. 80 (1998) 5357.
[52] B. Lauke, K. Grundke, DFG Project LA-818/11-1, Intermediate Report, 2002.
[53] G.H. Kelsall, S. Tang, S. Yurdakul, A.L. Smithm, J. Chem. Soc., Faraday Trans. 92 (1996) 3887.
[54] C.W. Extrand, Y. Kumagai, J. Colloid Interface Sci. 191 (1997) 378.